Published online 16 May 2017

Nucleic Acids Research, 2017, Vol. 45, No. 12 ***7261–7275***
doi: 10.1093/nar/gkx438

An intact Mcm10 coiled-coil interaction surface is important for origin melting, helicase assembly and the recruitment of Pol-α to Mcm2–7

Patricia Perez-Arnaiz, Irina Bruck, Max K. Colbert and Daniel L. Kaplan*

Florida State University College of Medicine, Department of Biomedical Sciences, Tallahassee, FL 32306, USA

Received December 14, 2016; Revised April 26, 2017; Editorial Decision April 27, 2017; Accepted May 03, 2017

ABSTRACT

Mcm10 is an essential eukaryotic factor required for DNA replication. The replication fork helicase is composed of Cdc45, Mcm2–7 and GINS (CMG). DDK is an S-phase-specific kinase required for replication initiation, and the DNA primase-polymerase in eukaryotes is pol α. Mcm10 forms oligomers *in vitro*, mediated by the coiled-coil domain at the N-terminal region of the protein. We characterized an Mcm10 mutant at the N-terminal Domain (NTD), Mcm10-4A, defective for self-interaction. We found that the Mcm10-4A mutant was defective for stimulating DDK phosphorylation of Mcm2, binding to eighty-nucleotide ssDNA, and recruiting pol α to Mcm2–7 *in vitro.* Expression of *wild-type* levels of *mcm10-4A* resulted in severe growth and DNA replication defects in budding yeast cells, with diminished DDK phosphorylation of Mcm2. We then expressed the *mcm10-4A* in *mcm5-bob1* mutant cells to bypass the defects mediated by diminished stimulation of DDK phosphorylation of Mcm2. Expression of *wild-type* levels of *mcm10-4A* in *mcm5-bob1* mutant cells resulted in severe growth and DNA replication defects, along with diminished RPA signal at replication origins. We also detected diminished GINS and pol-α recruitment to the Mcm2–7 complex. We conclude that an intact Mcm10 coiled-coil interaction surface is important for origin melting, helicase assembly, and the recruitment of pol α to Mcm2–7.

INTRODUCTION

The initiation of DNA replication is a cell cycle-regulated process that takes place in two temporally separated steps. The first step known as origin licensing involves the loading of the Mcm2–7 complex as a catalytically inactive double hexamer to encircle double-stranded DNA at origins of replication during late M and G_1 phases of the cell cycle. This reaction requires the action of accessory loading factors including ORC, Cdc6 and Cdt1 (1–3). During S phase, the S phase cyclin-dependent kinase (S-CDK) and the Dbf4-dependent Cdc7 kinase (DDK) trigger the second step of DNA replication known as origin firing. This step involves the assembly of the active replicative helicase (CMG complex), with the recruitment of Cdc45 and GINS to Mcm2–7 (4–8). The essential role of DDK in yeast is the phosphorylation of subunits of the Mcm2–7 complex (9–14). During S phase, the Mcm2–7 ring transitions from encircling dsDNA to encircling ssDNA (15). The active CMG encircles the leading strand and translocates away from the origin with 3′-5′ directionality (7,15,16).

Mcm10 is a non-enzymatic protein required for the initiation of DNA replication in eukaryotes (17–19,20). Mcm10 is loaded onto chromatin during G_1 in a Mcm2–7 dependent manner (21,22). Mcm10 has been proposed to have an essential role during helicase activation (19,20). One key event during DNA replication initiation is the recruitment of Cdc45 to the Mcm2 subunit, a member of the Mcm2–7 complex (5,23,24). Mcm10 plays a key role during DNA unwinding at origins of replication (9,25–28). Mcm10 may promote the ssDNA extrusion from the central channel of the Mcm2–7 ring by stimulating the DDK phosphorylation of Mcm2 during S phase (28). Moreover, expression of a mutant of Mcm10 defective for ssDNA interaction results in diminished recruitment of RPA to origins of replication, suggesting a role for Mcm10 in origin melting (29). In addition to its essential role during helicase activation, Mcm10 has been shown to link DNA unwinding and DNA synthesis (21) by helping the stabilization and recruitment of Pol-α to chromatin (21,30–33).

Mcm10 contains three functional domains: an N-terminal domain (NTD) involved in self-association (34–36), a highly conserved internal domain (ID) and a variable C-terminal domain (CTD) that is exclusive to metazoa (34). The ID has been implicated in the interaction with DNA and with different proteins including Mcm2–7, Pol-α and PCNA (31,37–40). The CTD is involved in DNA and Pol-α binding (38).

*To whom correspondence should be addressed. Tel: +1 850 645 0237; Fax: +1 850 644 5781; Email: Daniel.Kaplan@med.fsu.edu

Studies in *Xenopus laevis* Mcm10 have shown that dimer- and trimerization are mediated by an evolutionary conserved coiled-coil (CC) motif located in the first 100 amino acids of the protein (34,36). Mutations at specific residues of NTD CC region disrupted the self-association of Mcm10 *in vitro* and *in vivo* (36). Oligomerization has also been observed in human Mcm10 (41), consistent with a hexameric ring structure shown by electron microscopy (42). The Mcm10 NTD has also been implicated in the interaction of Mcm10 with the Mec3 subunit of the 9-1-1 clamp, in a region distinct from Mcm10's self-interaction domain (amino acids 100–150). This interaction may be indicating a role of Mcm10 in connecting DNA replication and DNA repair in yeast (43).

In this manuscript, we characterized an NTD Mcm10 mutant, Mcm10-4A, that is substantially defective in self-interaction, ssDNA binding, DDK stimulation and p180 recruitment to Mcm2–7 *in vitro*. Mcm10-4A is also modestly defective in dsDNA and Cdc7 binding *in vitro.* Expression of *mcm10-4A* in budding yeast confers a growth defect as a result of a defective DNA replication. When we expressed *mcm10-4A* in the *mcm5-bob1* genetic background the growth defect is not suppressed. Furthermore, expression of *mcm10-4A* in the *mcm5-bob1* background results in diminished replication protein A (RPA)-ChIP signal at origins of replication, delayed GINS-Mcm2–7 interaction and defective Pol12 recruitment *in vivo*. These data suggest that an intact Mcm10 coiled-coil interaction surface is important for helicase assembly, origin melting and for Pol-α recruitment to origins of replication in budding yeast cells.

MATERIALS AND METHODS

Cloning and purification of proteins

Full length *MCM10* PCR product was cloned into SpeI/XhoI sites of pET-41 vector and NdeI/XhoI sites of pET-33 vector to contain an N-terminal GST tag or a PKA tag respectively as described (44). The cloning of *MCM10* into pET-41 generates two-tagged protein (a GST tag at the N-terminus and a His tag at the C-terminus). We subcloned *MCM10* from pET-41-*MCM10* into the pRS415 plasmid. We used pET-41-MCM10, pET-33b-MCM10 and pRS415-MCM10 plasmids as templates to generate mutations in the MCM10 gene using Quick Change Site-directed Mutagenesis Kit (Agilent Technologies). GST-p180 was generated by cloning the full-length p180 gene into the pET-41 vector. Purification of *wild-type* and mutant GST-Mcm10 and GST-p180 proteins uses sequential nickel and glutathione resins. The details of GST-Mcm10 and PKA-Mcm10 are described (44). GST-Cdc45 was purified as described (45). Mcm2–7 proteins were purified and Mcm2–7 complex was assembled from recombinant subunits as described (13,46). GST-Dbf4 and GST-Cdc7 were purified a described (13). Protein kinase A was a generous gift from Susan Taylor.

DNA substrates and sequences

The sequences of the synthetic oligonucleotides used to prepare the DNA substrates are reported in Supplementary Table S1 (Supporting Material). Oligonucleotides were end labeled with T4 polynucleotide kinase (New England Biolabs) and radiolabeled ssDNA was purified over G-25 Sephadex Columns for Radiolabeled DNA Purification (Roche) according to manufacturer's instructions. To make double stranded (ds) DNA substrates, 4 μl of 500 nM radiolabeled ssDNA was incubated with 4 μl of 1 μM complementary DNA (1:2 molar ratio) and 4 μl of reaction buffer (20 mM Tris–HCl, 4% glycerol, 0.1 mM EDTA, 40 μg/ml BSA, 5 mM DTT and 10 mM magnesium acetate) in a final volume of 12 μl. The reaction was incubated 5 min at 95°C in a water bath, and then allowed to gradually cool down to 25°C. The reaction was then diluted with TE (20 mM Tris–HCl pH 8, 0.1 mM EDTA) to a final volume of 40 nM radiolabeled dsDNA.

Electrophoretic mobility shift assay (EMSA)

A standard DNA binding assay for EMSA analysis was performed in 20 μl containing 1 nM radiolabeled DNA, 20 mM Tris pH 7.5, 0.1 mM EDTA, 12% glycerol and 40 μg/ml BSA. The amount of Mcm10 added in each reaction is described in the figure. 1 nM of radiolabeled ssDNA was incubated with increasing amounts of protein at 4°C for 10 min in the electrophoretic mobility shift assays. The products of the assays were analyzed by 4% native PAGE followed by phosphorimaging. Results from similar experiments were quantified, averaged and plotted.

Kinase labeling of proteins

Kinase labeling was performed as described (44). Proteins with a PKA tag at the N-terminus (*wild-type* and mutant Mcm10, Mcm2 and Mcm2–7) were labeled in a reaction volume of 100 ul that contain 20 μM of PKA-tagged protein with 5 μg PKA in kinase reaction buffer (25 mM Tris–HCl pH 7.5, 5 mM DTT, 50 mM $MgCl_2$ and 500 μCi [γ-^{32}P]-ATP). The reaction was incubated at 30°C for 1 h.

GST pulldown assay

The GST pulldown assays were performed as described (44). GST-tagged protein attached to Glutathione Sepharose (GE Healthcare) previously equilibrated with GST binding buffer (40 mM Tris–HCl pH 7.5, 100 mM NaCl, 0.1 mM EDTA, 10% glycerol, 0.1% Triton X-100, 1 mM DTT, 0.7 μg/ml pepstatin, 0.1 μg/ml leupeptin, 0.1 mM PMSF and 0.1 mg/ml BSA) was incubated with varying concentrations of radiolabeled protein in GST binding buffer in a final reaction volume of 100 μl. The reactions were incubated at 30°C for 10 min with gentle mix every few minutes. When the binding was complete, the reactions were shifted to room temperature and glutathione beads were allowed to settle. The supernatant was removed and the beads were washed two times with 500 μl GST binding buffer. After the last wash, beads were heated at 90°C for 10 min in SDS-sample buffer (2% SDS, 4% glycerol, 4 mM Tris–HCl, 2 mM DTT and 0.01% bromophenol blue). The reactions were then analyzed by SDS-PAGE followed by phosphorimaging and quantification.

DDK phosphorylation assay

Kinase reactions were performed in a volume of 25 μl and contained 25 mM HEPES–NaOH pH 7.5, 1 mM DTT,

10 mM magnesium acetate, 75 mM sodium acetate, 5 mM ATP, 0.1 mg/ml BSA, 1 mM sodium fluoride, 0.1 mM Na_3VO_4, 5 μg Mcm2 and 50 ng DDK. The amount of Mcm10 added in each reaction is described in the figure. Reactions were incubated at 30°C for 1 h. Reactions were stopped by addition of SDS-sample buffer and analyzed by Western blot using an antibody against Mcm2-164-phosphoserine-170-phosphoserine.

Yeast strains and cell growth

All yeast strains used in this study are shown in Supplementary Table S2. The *mcm10-1*-aid strains were obtained from Yeast Genetic Resource Center. The *mcm5-bob1* strain was obtained from Robert A. Sclafani (47). The *mcm10-1*-aid *mcm5-bob1* strain was constructed by yeast mating (using strains BY25926 and RSY728), sporulation and tetrad analysis. The presence of *mcm5-bob1* mutation was confirmed by survival at the restrictive temperature of 37°C after Cdc7 deletion. The *cdc7* deletion mutation *cdc7Δ::Trp1* was created by PCR-based gene disruption technique and confirmed by PCR. The strain that grew at 37°C after Cdc7 deletion was then sequenced to confirm the presence of *mcm5-bob1*. Yeast transformation was carried out by either electroporation (plasmid DNA) or the lithium acetate procedure (linear DNA) (48). In all experiments cells were grown at 25°C to slow down replication dynamics as described before (21). *mcm10-1*-aid and *mcm10-1*-aid *mcm5-bob1* strains carrying plasmids for exogenous expression of *wild-type mcm10* and *mcm10-4A* were grown overnight in CSM-Leu media supplemented with 2% raffinose. *Wild-type* and mutant Mcm10 proteins were overexpressed in YPGal media from galactose-inducible promoter in the presence of 500 μM IAA (Sigma) to induce the degradation of endogenous *MCM10* gene. *mcm10-1*-aid and *mcm10-1*-aid *mcm5-bob1* strains carrying plasmids for exogenous expression of *MCM2-WT* and *mcm2-S164A-S170A* were grown overnight in CSM-Leu media supplemented with 2% raffinose. *MCM2-WT* and *mcm2-S164A-S170A* proteins were overexpressed in YPGal media from galactose-inducible promoter.

Plasmids

The following plasmids were used in this study: pPP13 (pRS415 CEN6/ARSH4 GALS::MCM10 LEU2), pPP31 (pRS415 CEN6/ARSH4 GALS::mcm10I26A L30A R37A L40A LEU2), pIB302 (pRS415 CEN6/ARSH4 GALS::MCM2 LEU2), pIB305 (pRS415 CEN6/ARSH4 GALS::mcm2S164A S170A LEU2).

Yeast serial dilution analysis

Serial dilution was performed as described (49). 10-fold serial dilution was performed and spotted on the indicated media and incubated at 25°C for 3 days.

Co-immunoprecipitation

Cells were grown overnight in CSM-Leu containing raffinose (2%) at 25°C. When the cell density reached 6×10^6 cells, the cells were spun down and resuspended in YP-Gal (0.15% galactose) in the presence of 500 μM IAA and α-factor (Zymo Research). The cells were grown for 3 h at 25°C, spun down, washed three times and resuspended in fresh, pre-warmed YPGal with 500 μM IAA. Cells were further incubated at 25°C for the indicated times. Co-immunoprecipitation was performed as described (50). Cells were collected and lysed at 4°C with acid-washed glass beads (Sigma) in IP buffer [100 mM HEPES–KOH pH 7.9, 100 mM potassium acetate, 10 mM magnesium acetate, 2 mM sodium fluoride, 0.1 mM Na_3VO_4, 20 mM β-glycerophosphate, 1% Triton X-100, 0.7 μg/ml pepstatin, 0.1 μg/ml leupeptine, 0.1 mM PMSF, 1× complete protease inhibitor cocktail without EDTA (Roche)] using a BeadBeater. Lysed material was treated with 200 U of Benzonase (Novagen) at 4°C for 30 min. Clarified extracts were then mixed with 2 μl of specific antibody and rotated for 2 h at 4°C. Following this, 50 μl of Protein G Sepharose beads (GE Healthcare) equilibrated in IP buffer were added to the extracts and further rotated for 1 h at 4°C. Beads were washed twice with IP buffer and finally resuspended in SDS-sample buffer. Western analysis was performed with antibody directed against relevant epitope tags, and blots were scanned using the LI-COR Odyssey Infrared Imager and analyzed and quantified in the Image Studio 4.0 Software.

Chromatin immunoprecipitation

Cells initially cultured in CSM-Leu were treated with α-factor and 500 μM IAA in YPGal for 3 h at 25°C. Following extensive washes, cells were further incubated and time course samples were taken at the indicated points. Chromatin immunoprecipitation was performed as described (45). Formaldehyde cross-linked cells were lysed with acid-washed glass beads in a BeadBeater. DNA was fragmented by sonication (Branson 450, 5 cycles of 15 s. each). RPA (2 μl) antibody and magnetic protein A beads (Dynalbeads Protein A, Invitrogen) were added to the cleared lysate to immunoprecipitate DNA. Immunoprecipitates were then washed extensively to remove nonspecific DNA. Eluted DNA was subjected to PCR analysis using primers directed against *ARS306* or a midway between *ARS305* and *ARS306* as described (26). We performed PCR with [^{32}P-α]-dCTP as a component of the PCR reaction to quantify the amplified product. The radioactive band in the native gel, representing specific PCR amplified DNA product, was quantified by phosphorimaging and normalized by a reference standard (a PCR reaction with a known quantity of template DNA) run in the same gel.

Fluorescence activated cell sorting (FACS)

Samples were fixed with 70% ethanol and FACS was performed as described previously (49). Cells initially cultured in CSM-Leu were treated with α-factor and 500 μM IAA in YPGal for 3 h at 25°C. After extensive washes, cells were incubated for the indicated times and stained with propidium iodide. Cell cycle progression data were obtained using BD FACS Canto Ruo Special Order System and analyzed using FACS Diva software.

Antibodies

Antibodies against Mcm10, Mcm2 and Mcm2-phosphoserine-164-phosphoserine-170-phosphoserine, Cdc45, GINS and Pol12 were supplied by Open Biosystems (we supplied the antigens). Crude serum was purified against immobilized antigen to remove nonspecific antibodies. The specificity of each antibody was analyzed by Western blot of purified proteins and yeast extract. Antibodies directed against RPA (Thermo Scientific), FLAG epitope (Sigma) and Arp3 (Santa Cruz Biotechnology) were commercially purchased. Antibodies against epitope tags in the co-immunoprecipitation experiments were obtained from Sigma.

RESULTS

Mutations in the NTD coiled-coil region disrupts the self-association of Mcm10 in vitro

Studies in yeast and *X. laevis* showed that Mcm10 has the ability for oligomerization. This self-interaction is mediated by the coiled-coil region belonging to the NTD (34,36). We introduced mutations at specific residues of *Saccharomyces cerevisiae* Mcm10 that were previously found to be important for self-interaction *in vitro* and *in vivo* in *X. laevis* Mcm10 (36). We eliminated side chains at residues Ile26, Leu30, Arg37 and Leu40 by alanine substitution to create a Mcm10-I26A-L30A-R37A-L40A quadruple mutant (Mcm10-4A) (Figure 1A). We purified and tested Mcm10-4A mutant for self-interaction *in vitro* by using a GST pulldown assay. We incubated *wild-type* GST-Mcm10, GST-Mcm10-4A or GST-Tag alone with increasing amounts of radiolabeled *wild-type* PKA-Mcm10 and PKA-Mcm10-4A. We found that *wild-type* Mcm10 showed a strong self-interaction (Figure 1B). In contrast, the interaction of *wild-type* Mcm10 with Mcm10-4A was severely decreased. Furthermore, the interaction of Mcm10-4A with itself showed a signal at background levels (Figure 1B). These data indicate that self-interaction is severely impaired in the Mcm10 NTD mutant.

We also wanted to test another NTD mutant previously shown to be important for self-interaction *in vitro* and *in vivo* in *X. laevis* Mcm10 (36). For that purpose, we substituted Ile26 and Leu30 with aspartate to create a Mcm10-I26D-L30D double mutant (Mcm10-2D) (Figure 1A). Next, we purified the mutant protein and tested it for Mcm10 interaction *in vitro* using a GST pulldown assay. We found that Mcm10-2D was defective in the interaction with both *wild-type* Mcm10 and Mcm10-4A (Supplementary Figure S1A). Furthermore, the self-interaction of Mcm10-2D showed a background level signal (Supplementary Figure S1A). We found that this mutant was also substantially defective in ssDNA, dsDNA and Mcm2–7 binding (Supplementary Figure S1). Since we were looking for a separation-of-function mutation, we did not study this mutant any further.

Mcm10-4A is defective in 80mer ssDNA binding *in vitro*

Previous studies showed that Mcm10 is able to bind both single- (ss) and double-stranded (ds) DNA (37,51). Furthermore, a previous study in yeast showed that multiple copies

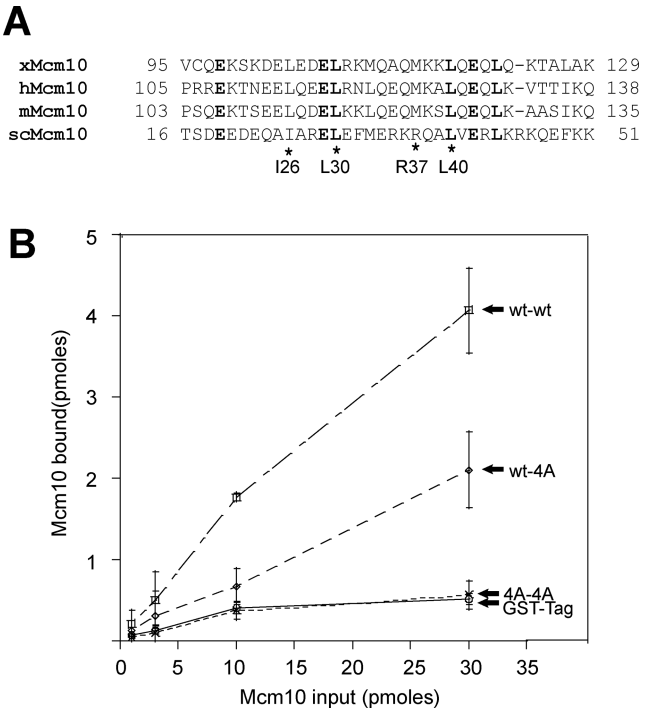

Figure 1. Mutations at residues belonging to Mcm10 NTD coiled-coil region disrupts Mcm10 self-association *in vitro*. (**A**) Sequence alignment of the coiled-coil region from *Xenopus laevis* (x), *Homo sapiens* (h), *Mus musculus* (m) and *Saccharomyces cerevisiae* (sc) (36). Bold letters indicate identical aminoacids. Residues 16–51 from *S. cerevisiae* are shown. Ile26, Leu30, Arg37 and Leu40 were targeted for site-directed mutagenesis. (A and B) Mcm10-4A is Mcm10-I26A-L30A-R37A-L40A. (**B**) 30 pmol of *wild-type* GST-Mcm10, GST-Mcm10-4A or GST tag was incubated with increasing concentrations of either radiolabeled *wild-type* PKA-Mcm10 or PKA-Mcm10-4A at 30°C for 10 min in a GST pulldown assay. The products of the pulldown were analyzed by SDS-PAGE followed by phosphorimaging. Results from similar experiments were quantified, averaged and plotted. The graph represents mean values from two independent experiments and error bars indicate the standard deviation of the mean.

of Mcm10 are able to bind to long DNAs, with the number of Mcm10 molecules directly proportional to the length of the DNA (51).

We wanted to determine if purified Mcm10-4A mutant was able to bind DNA *in vitro*. For that purpose we performed a GST pulldown assay in which we used 80 nucleotide or 25-nucloeitde ssDNA, dsDNA, or a partially unwound dsDNA (bubble DNA). We incubated GST-Mcm10, GST-Mcm10-4A or GST-Tag with increasing amounts of radiolabeled ssDNA, dsDNA or bubble DNA. We found that *wild-type* Mcm10 interacted stably with all DNA substrates. Mcm10-4A was substantially defective in binding 80-nucleotide ssDNA and bubble DNA (Figure 2A and B). In contrast, the Mcm10 mutant is only partially defective in dsDNA binding (Figure 2C), and not defective at all for 25-nucleotide ssDNA binding (Figure 2D). These data suggest that Mcm10 self-interaction and oligomerization may be important for the interaction of Mcm10 with 80 nucleotide ssDNA or bubble-DNA, consistent with previous studies (51).

To study the process of association of *wild-type* and mutant Mcm10 purified proteins with DNA, we performed an

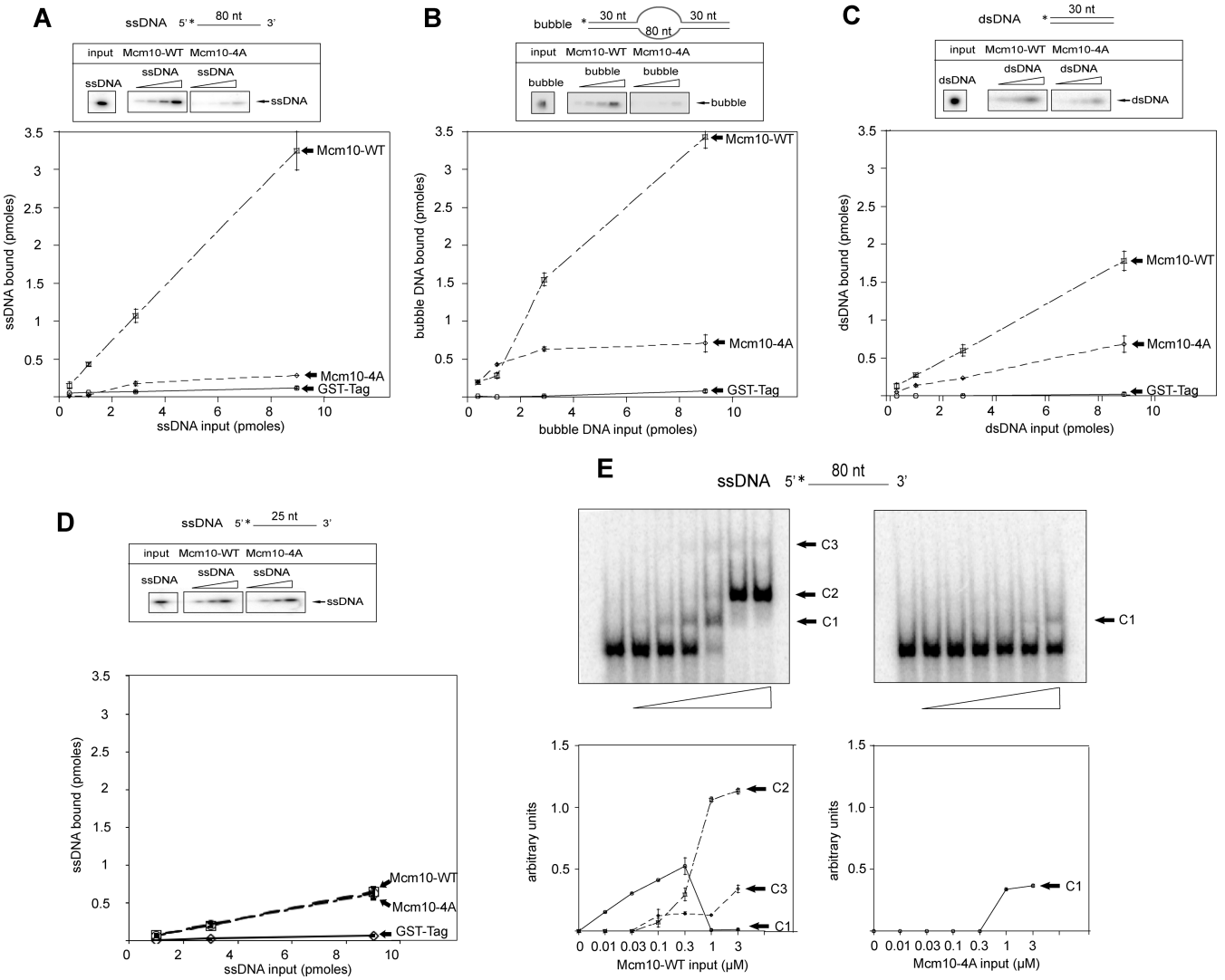

Figure 2. Mcm10-4A is defective in 80mer ssDNA binding *in vitro.* (**A**) 30 pmol of *wild-type* GST-Mcm10, GST-Mcm10-A4 or GST tag was incubated with increasing concentrations of radiolabeled 80mer ssDNA at 30°C for 10 min in a GST pulldown assay. The products of the pulldown were analyzed by SDS-PAGE followed by phosphorimaging. Results from similar experiments were quantified, averaged and plotted. (**B**) 30 pmol of *wild-type* GST-Mcm10, GST-Mcm10-A4 or GST tag was incubated with increasing concentrations of radiolabeled bubble DNA at 30°C for 10 min in a GST pulldown assay. The products of the pulldown were analyzed by SDS-PAGE followed by phosphorimaging. Results from similar experiments were quantified, averaged and plotted. (**C** and **D**) 30 pmol of *wild-type* GST-Mcm10, GST-Mcm10-A4 or GST tag was incubated with increasing concentrations of radiolabeled 30mer dsDNA (C) or 25mer ssDNA (D) at 30°C for 10 min in a GST pulldown assay. The products of the pulldown were analyzed by SDS-PAGE followed by phosphorimaging. Results from similar experiments were quantified, averaged and plotted. (**E**) 1 nM of radiolabeled ssDNA was incubated with increasing amounts of GST-Mcm10 and GST-Mcm10-4A at 4°C for 10 min in an electrophoretic mobility shift assays. The products of the assays were analyzed by 4% native PAGE followed by phosphorimaging. Results from similar experiments were quantified, averaged and plotted. Graphs from (A), (B), (C), (D), and (E) represent mean values from two independent experiments and error bars indicate the standard deviation of the mean.

electrophoretic mobility gel shift assay. This *in vitro* DNA binding assay offers the advantage to resolve complexes of different conformation or stoichiometry. The analysis was performed using a radiolabeled 80-mer ssDNA and increasing amounts of *wild-type* or mutant Mcm10 purified proteins. In the case of *wild-type* Mcm10, we were able to detect different retardation bands as we increased the concentration of Mcm10 added to the reaction. The appearance of slower moving bands is concomitant with the disappearance of free DNA and directly proportional to the Mcm10 amount added to the reaction (Figure 2E, left panel). This result can be explained if the different retarded bands correspond to distinct protein–DNA complexes formed in which ssDNA is associated with a different number of Mcm10 molecules. In contrast, Mcm10-4A produces a faint single-retardation band at the highest Mcm10 concentration assayed (Figure 2E, right panel). This complex likely corresponds to a complex formed by ssDNA and a single Mcm10 molecule. These results indicate that the NTD Mcm10 mutant is defective in oligomerization and that this ability is importantfor the interaction of Mcm10 with 80 nt single-stranded DNA.

Mcm10-4A is not defective in binding Mcm2–7 *in vitro*

It has previously shown that Mcm10 interacts with Mcm2–7 *in vivo* and *in vitro* (18,22,26,28,40,52). We wanted to determine the role of the Mcm10 NTD on Mcm10-Mcm2–7 interaction. We incubated GST-Mcm10, GST-Mcm10-4A or GST-Tag alone with increasing amounts of radiolabeled PKA-Mcm2–7 and performed a GST pulldown assay. We found that Mcm10-4A is able to bind Mcm2–7 as *wild-type* Mcm10 (Figure 3A), indicating that Mcm10 NTD is not involved in Mcm2–7 binding *in vitro.*

Mcm10-4A binds and recruits Cdc45 to the Mcm2–7 complex like Mcm10-WT *in vitro*

Mcm10 has been shown to recruit Cdc45 onto chromatin (30,28,53,54). To investigate whether Mcm10-4A recruits Cdc45 to Mcm2–7, first we examined whether Mcm10 mutant binds directly to Cdc45. We used a GST pulldown analysis in which we incubated GST-Cdc45 with radiolabeled *wild-type* and mutant PKA-Mcm10 proteins. Mcm10-4A showed a Cdc45 binding similar to *wild-type* Mcm10 (Figure 3B). To test whether Mcm10 mutant can recruit Cdc45 to Mcm2–7, we next incubated GST-Cdc45 with a fixed amount of radiolabeled PKA-Mcm2–7 and increasing concentrations of radiolabeled *wild-type* and mutant PKA-Mcm10 proteins. We observed that the amount of Cdc45 bound to Mcm2–7 substantially increased as we added increasing concentrations of *wild-type* Mcm10 or Mcm10-4A to the reaction (Figure 3C). These data indicate that Mcm10-4A can recruit Cdc45 to the Mcm2–7 complex *in vitro* and that NTD is not involved in this recruitment.

Mcm10-4A is defective in stimulating Mcm2 phosphorylation by DDK in vitro

We previously found that Mcm10 interacts with DDK and stimulates the phosphorylation of Mcm2 *in vitro* (28). Furthermore, in the absence of Mcm10, cells show a modestly decrease Mcm2 phosphorylation *in vivo* (28). We first determined using purified proteins if there are direct interactions between Mcm10 mutants and both DDK subunits: the regulatory Dbf4 and the catalytic Cdc7. We incubated GST-Dbf4, GST-Cdc7 or GST-tag with increasing amounts of radiolabeled *wild-type* PKA-Mcm10 and PKA-Mcm10-4A. Mcm10-4A shows a slightly reduced Dbf4 interaction and a substantially reduced Cdc7 binding capacity compared to *wild-type* Mcm10 (Figure 4A and B). These data suggest that Mcm10 oligomerization through the NTD is not necessary for Dbf4 interaction, but it may be important for Cdc7 binding.

We then investigated the ability of Mcm10-4A to stimulate Mcm2 phosphorylation by DDK *in vitro*. We performed an *in vitro* kinase assay in which we incubate Mcm2 with DDK and increasing amounts of *wild-type* Mcm10 or Mcm10-4A at 30°C for 1 h. We examined the levels of phospho-Mcm2 with an antibody directed against Mcm2-phosphoserines 164 and 170 (13,14). DDK phosphorylates Mcm2 weakly *in vitro* (13). We found a substantial increase in Mcm2 phosphorylation as we added *wild-type* Mcm10 to the reaction (Figure 4C, left panel) as it was shown before (28). We detected some phosphoMcm2 signal at the no-DDK point for *wild-type* Mcm10 (Figure 4C, left panel). It may be the result of some weak cross-reactivity between the phospho-antibody and unphosphorylated Mcm2. In the case of Mcm10 mutant, the amount of phospho-Mcm2 is slightly increased at the highest Mcm10-4A concentration assayed (Figure 4C, right panel), but this amount of phospho-Mcm2 is reduced compared to *wild-type* Mcm10 (Figure 4C). This result indicates that Mcm10-4A is defective in stimulating DDK phosphorylation of Mcm2 *in vitro*.

Mcm10-4A is substantially defective for p180 recruitment to Mcm2–7 *in vitro*

It has previously been shown that Mcm10 helps recruit pol-α to origins of replication (21,30). Mcm10 interacts through its ID with p180 (34,38), the subunit that contains the catalytic DNA polymerase activity of pol-α (55). We wanted to test if the Mcm10-4A mutant is able to interact with p180 *in vitro* using a GST pulldown assay. We incubated GST-p180 or GST-Tag alone with increasing amounts of either radiolabeled PKA-Mcm10–WT or PKA-Mcm10-4A. Mcm10-4A exhibited a very slight defect in p180 interaction compared to Mcm10-WT (Figure 5A). Next, we determined whether Mcm10-4A was defective in recruiting p180 to Mcm2–7 *in vitro* using the GST pulldown assay. We found that, for *wild-type* Mcm10, increasing concentrations of Mcm10 stimulated the interaction between GST-p180 and PKA-Mcm2–7 (Figure 5B). However, for Mcm10-4A, there was little interaction between GST-p180 and PKA-Mcm2–7, even at the highest concentration of Mcm10-4A (Figure 5B). Since the direct interaction between Mcm10-4A and both Mcm2–7 and p180 are close to *wild-type* levels (Figures 3A and 5A), whereas the recruitment of p180 to Mcm2–7 is substantially defective for Mcm10-4A (Figure 5B), the data suggest that an intact Mcm10 coiled-coil interaction surface is important for the recruitment of p180 to Mcm2–7 *in vitro*.

Then we studied the recruitment of p180 to the different isolated Mcm2–7 subunits by Mcm10. We found that *wild-type* Mcm10 exhibits substantial recruitment of p180 to Mcm2 and Mcm7 and modest recruitment to Mcm4 (Figure 5C). Thus, we next determined whether an intact Mcm10 coiled-coil interaction surface is important for p180 recruitment to the Mcm2, Mcm4 and Mcm7 subunits. Unlike *wild-type* Mcm10, the Mcm10-4A mutant was defective for p180 recruitment to each of these three subunits, with the largest defect observed for Mcm2 recruitment (Figure 5D–F). These data suggest that an intact Mcm10 coiled-coil interaction surface is important for p180 recruitment to the Mcm2 subunit of the Mcm2–7 complex, while recruitment of p180 to Mcm4 or Mcm7 subunits is also possible.

Expression of mcm10-4A results in a growth defect and slowed progression through S phase

To investigate the role of Mcm10 mutants *in vivo* we used an IAA-inducible degron *(mcm10-1*-aid) in which the genomic copy of *MCM10* is degraded upon de addition of IAA to the culture media (27,56). We constructed plasmids with *wild-type MCM10* and *mcm10-4A* under the control of GalS promoter, a low-copy inducible expression system

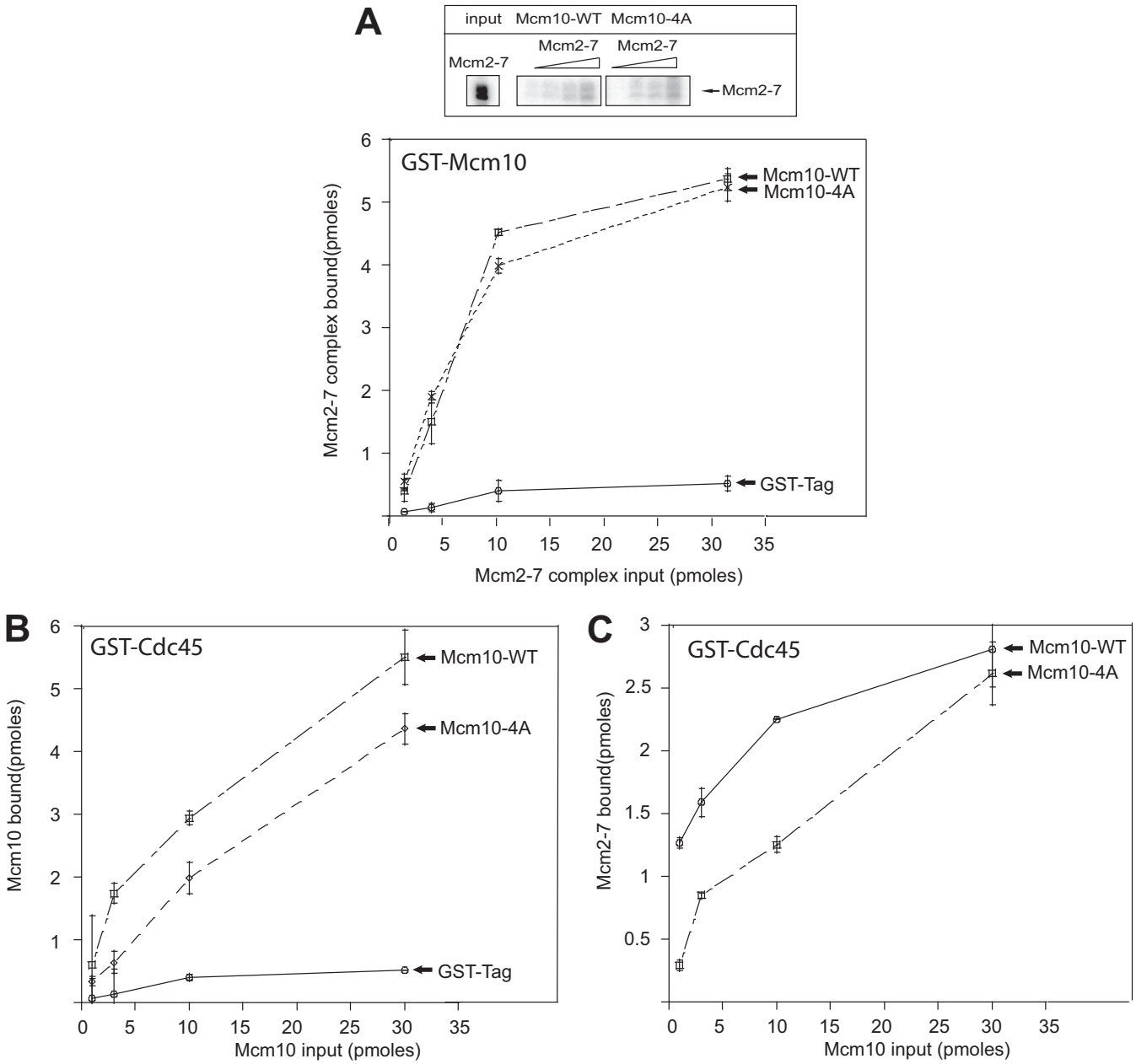

Figure 3. Mcm10-4A is able to bind and recruit Cdc45 to the Mcm2–7 complex *in vitro*. (**A**) 30 pmol of *wild-type* GST-Mcm10, GST-Mcm10-A4 or GST tag was incubated with increasing concentrations of radiolabeled PKA-Mcm2–7 at 30°C for 10 min in a GST pulldown assay. The products of the pulldown were analyzed by SDS-PAGE followed by phosphorimaging. Results from similar experiments were quantified, averaged and plotted. (**B**) 30 pmol of GST tag or GST-Cdc45 was incubated with varying amounts of radiolabeled *wild-type* PKA-Mcm10 or PKA-Mcm10-4A in a GST pulldown assay. The products of the pulldown were analyzed by SDS-PAGE followed by phosphorimaging. Results from similar experiments were quantified, averaged and plotted. (**C**) 30 pmol of GST-Cdc45 was incubated with 10 pmol of radiolabeled PKA-Mcm2–7 and increasing amounts of *wild-type* Mcm10 or Mcm10-4A in a GST pulldown assay. The products of the pulldown were analyzed by SDS-PAGE followed by phosphorimaging. Results from similar experiments were quantified, averaged and plotted. Graphs from (A), (B) and (C) represent mean values from two independent experiments and error bars indicate the standard deviation of the mean.

(57). These plasmids were then transformed into *mcm10-1*-aid strain. In the absence of IAA and galactose (permissive conditions), only the genomic copy of *MCM10* is expressed. Under these conditions, cells harboring plasmids with *MCM10-WT*, empty vector and *mcm10-4A* each grow similarly as analyzed by serial 10-fold dilutions on agar plates (Figure 6A, left panel). This result was expected because, in the absence of galactose, no *mcm10* mutant was induced. However, once IAA and galactose are added (restrictive conditions), the genomic copy of *MCM10* is degraded and the plasmid copy of *mcm10* is expressed. We varied levels of galactose to achieve equal Mcm10 expression levels of *mcm10-4A* (degron on) compared to *wild-type* cells (degron off) (Supplementary Figure S2). We next performed a similar experiment in the presence of IAA and galactose. Under these conditions, cells expressing *mcm10-4A* exhibited a

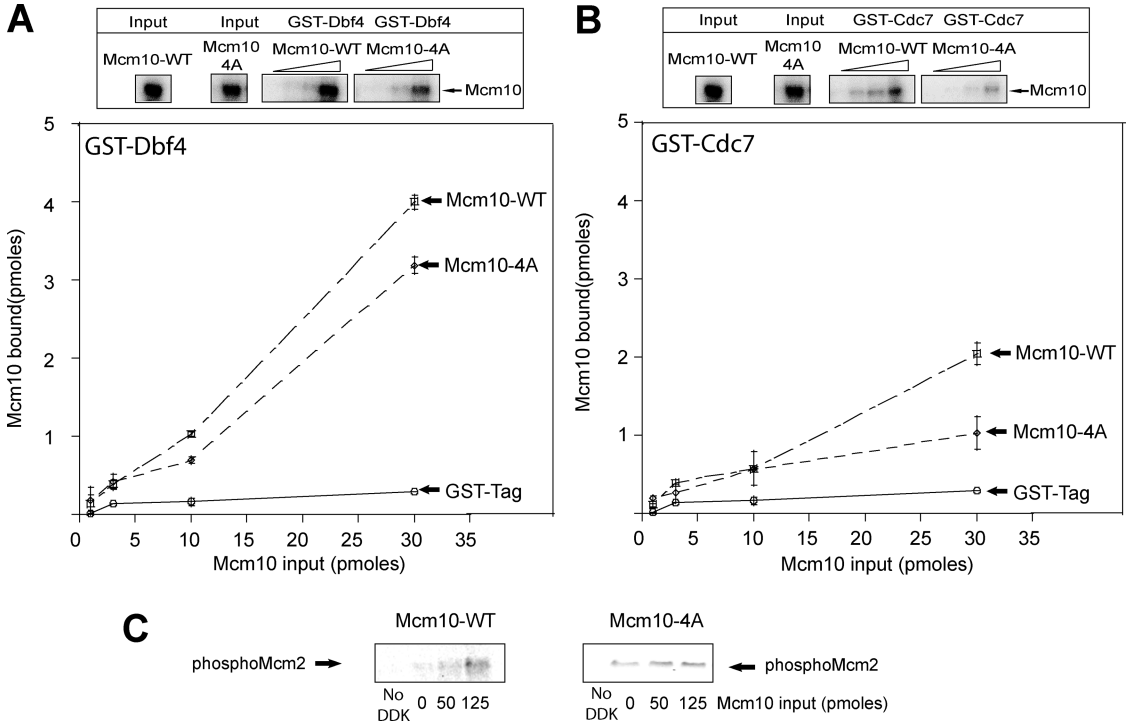

Figure 4. Mcm10-4A is slightly defective in stimulating Mcm2 phosphorylation by DDK *in vitro*. (**A**) 30 pmol of GST-Dbf4 or GST tag was incubated with increasing concentrations of radiolabeled *wild-type* PKA-Mcm10 or PKA-Mcm10-4A at 30°C for 10 min in a GST pulldown assay. The products of the pulldown were analyzed by SDS-PAGE followed by phosphorimaging. Results from similar experiments were quantified, averaged and plotted. (**B**) 30 pmol of GST-Cdc7 or GST tag was incubated with increasing concentrations of either radiolabeled *wild-type* PKA-Mcm10 or PKA-Mcm10-4A at 30°C for 10 min in a GST pulldown assay. The products of the pulldown were analyzed by SDS-PAGE followed by phosphorimaging. Results from similar experiments were quantified, averaged and plotted. (**C**) 5 μg of Mcm2 was incubated with 50 ng of DDK and varying amounts of *wild-type* Mcm10 or Mcm10-4A in a volume of 25 μl at 30°C for 1 h. The reactions were then analyzed by western blot for expression of phospho-Mcm2. Graphs from (A) and (B) represent mean values from two independent experiments and error bars indicate the standard deviation of the mean.

growth defect (Figure 6A, right panel). These data suggest that the Mcm10 NTD is important for budding yeast cell growth on agar plates.

To characterize the effect of the Mcm10 NTD mutations during DNA replication, we subjected *MCM10-WT* and *mcm10-4A* to FACS analysis. We found a slow progression through S phase for cells expressing *mcm10* mutant (Figure 6B).

Cells expressing mcm10-4A are slightly defective for DDK phosphorylation of Mcm2

It has been previously described that the phosphorylation of Mcm2 by DDK may be responsible for the ssDNA extrusion from the central ring of the Mcm2–7 ring (14). We found that Mcm10-4A is defective in DDK stimulation of Mcm2 *in vitro* (Figure 4C). We next analyzed the levels of phospho-Mcm2 in cells expressing Mcm10 mutants. For that, we use an antibody directed against the DDK sites on Mcm2 (anti-Mcm2-phosphoS164-phospho170) (13,14). We arrested cells in G_1 with α–factor under restrictive conditions for 3 hours and then release them into growth media lacking α-factor under the restrictive conditions for 0, 15, 30 and 45 min. We made whole cell extracts and found that cells expressing *mcm10-WT* showed an increase in phospho-Mcm2 signal as cells entered S phase (Figure 6C, bottom left panel). Cells expressing *mcm10-4A* exhibited similar levels of phosphoMcm2 signal compared to *wild-type* at 30 min during S phase. At 45 min the level of phosphor-Mcm2 is slightly decreased in *mcm10-4A* mutant (Figure 6C, bottom right panel). These results suggest that expression of *mcm10-4A* confers a slight decrease in Mcm2 phosphorylation by DDK *in vivo*.

The presence of mcm5-bob1 mutation does not suppress the growth defect observed in mcm10-4A

The *mcm5-bob1* mutation is able to suppress the growth defect observed when *cdc7* is deleted from the budding yeast genome (58). *mcm5-bob1* also suppresses the severe growth defect conferred by a mutant of Mcm2 (*mcm2-S164A-S170A*) that is not phosphorylated by DDK (14). We wanted to study the effect of the expression of *mcm10-4A* in *mcm10-1*-aid cells harboring the *mcm5-bob1* genetic background. We transformed *mcm10-1*-aid *mcm5-bob1* cells with our galactose inducible *MCM10-WT* and *mcm10-4A*. The growth defect observed when *mcm10-4A* mutant is expressed under restrictive conditions (Figure 7A) was not at all suppressed by the presence of *mcm5-bob1* mutation (Figure 7B). As a control, we transformed *mcm10-1*-aid strains with a plasmid expressing the phosphodead Mcm2 mutant (*mcm2-S164A-S170A*). The severe growth defect shown by this mutant is suppressed by the presence of the *mcm5-bob1* mutation (Supplementary Figure S3).

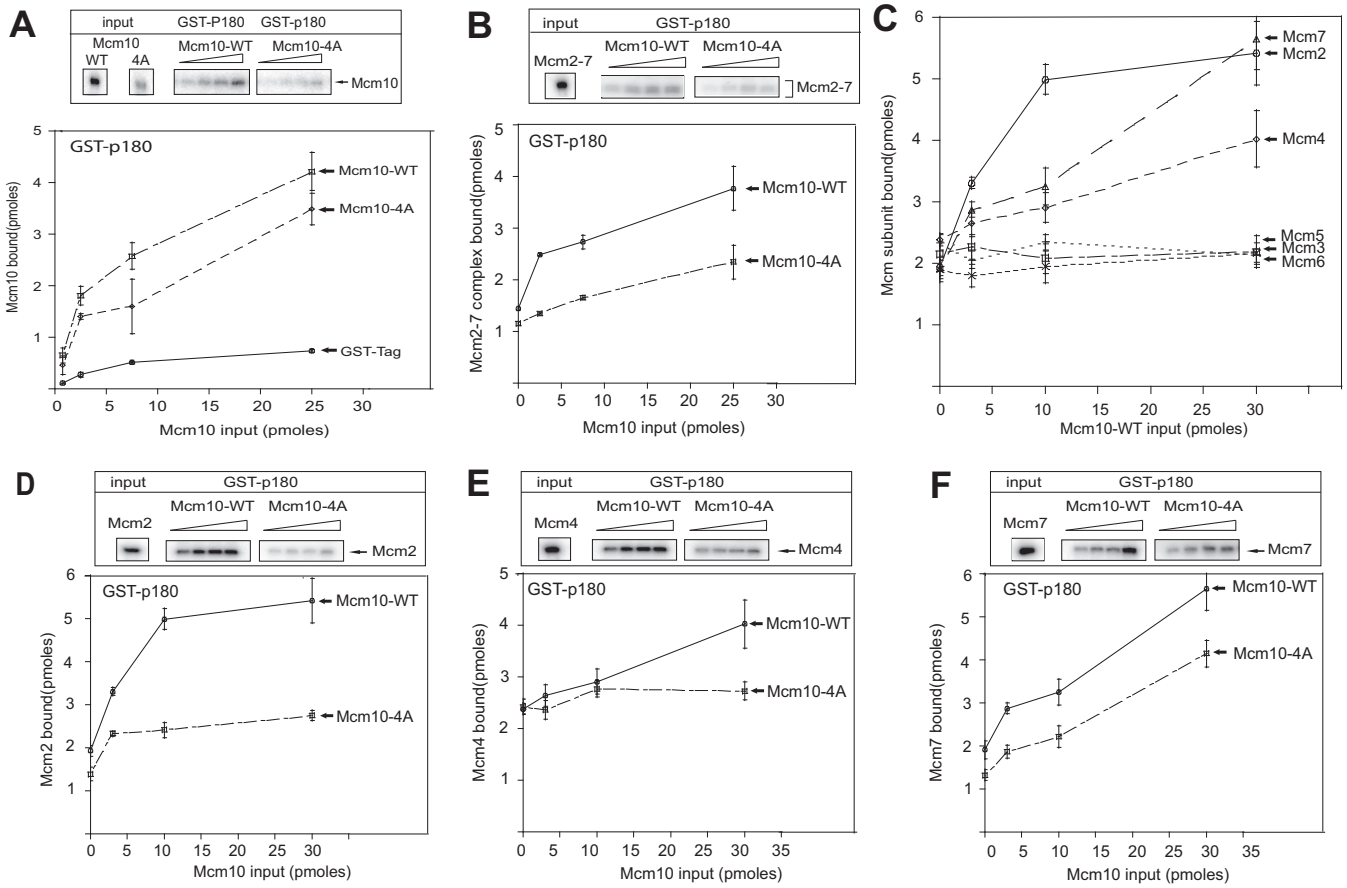

Figure 5. Mcm10-4A is slightly defective in p180 binding *in vitro*. (**A**) 30 pmol of GST-p180 or GST tag was incubated with increasing concentrations of either radiolabeled PKA-Mcm10-WT or PKA-Mcm10-4A at 30°C for 10 min in a GST pulldown assay. The products of the pulldown were analyzed by SDS-PAGE followed by phosphorimaging. Results from similar experiments were quantified, averaged and plotted. (**B**) 30 pmol of GST-p180 was incubated with 10 pmoles of radiolabeled PKA-Mcm2–7 and increasing amounts of *wild-type* Mcm10 or Mcm10-4A in a GST pulldown assay. The products of the pulldown were analyzed by SDS-PAGE followed by phosphorimaging. Results from similar experiments were quantified, averaged and plotted. (**C**) 30 pmol of GST-p180 was incubated with 10 pmol of the isolated radiolabeled PKA-Mcm2–7 subunits and increasing amounts of *wild-type* Mcm10 in a GST pulldown assay. The products of the pulldown were analyzed by SDS-PAGE followed by phosphorimaging. Results from similar experiments were quantified, averaged and plotted. (**D**) 30 pmol of GST-p180 was incubated with 10 pmol of radiolabeled PKA-Mcm2 and increasing amounts of *wild-type* Mcm10 or Mcm10-4A in a GST pulldown assay. The products of the pulldown were analyzed by SDS-PAGE followed by phosphorimaging. Results from similar experiments were quantified, averaged and plotted. (**E**) 30 pmol of GST-p180 was incubated with 10 pmol of radiolabeled PKA-Mcm4 and increasing amounts of radiolabeled *wild-type* PKA-Mcm10 or PKA-Mcm10-4A in a GST pulldown assay. The products of the pulldown were analyzed by SDS-PAGE followed by phosphorimaging. Results from similar experiments were quantified, averaged and plotted. (**F**) 30 pmol of GST-p180 was incubated with 10 pmol of radiolabeled PKA-Mcm7 and increasing amounts of radiolabeled *wild-type* PKA-Mcm10 or PKA-Mcm10-4A in a GST pulldown assay. The products of the pulldown were analyzed by SDS-PAGE followed by phosphorimaging. Results from similar experiments were quantified, averaged and plotted.

We also compared growth rate of *mcm10-4A* to *mcm10-Δ1-100* using serial dilution on agar plates (Supplementary Figure S4). In these experiments, MCM10 was expressed from either the GAL S promoter or native promoter. In either case, we found that expression of *mcm10*-4A resulted in a severe growth defect, and this growth defect was nearly identical to the growth defect conferred by expression of *mcm10-Δ1-100.* These data further support that an intact Mcm10 coiled-coil interaction surface is important for cell growth. Three previous *in vivo* studies show that deletion of the N-terminal 100 amino acids of Mcm10 does not affect cell growth (43,52,59). However, these studies used different strain backgrounds and different methods to degrade endogenous Mcm10 compared to this study. Thus, the relative importance of the N-terminus of Mcm10 on cell growth depends upon the strain background and experimental conditions.

We next studied whether cells expressing *mcm10-4A* in a *mcm5-bob1* background under restrictive conditions exhibited a defect in RPA-ChIP signal at origins of replication. For that purpose, we synchronized cells in G_1 with α-factor in the presence of IAA and then released them into medium lacking α-factor for 0, 15, 30, 45 and 60 min. Then we performed chromatin immunoprecipitation with antibodies against yeast RPA, followed by quantitative PCR probing for origin (*ARS306*) and non-origin (region between *ARS305* and *ARS306*) sequences. An increased signal was observed for cells expressing *mcm10-WT* during S phase (Figure 7C, left panel), indicating active origin melting/DNA unwinding. At 60 min we observed a de-

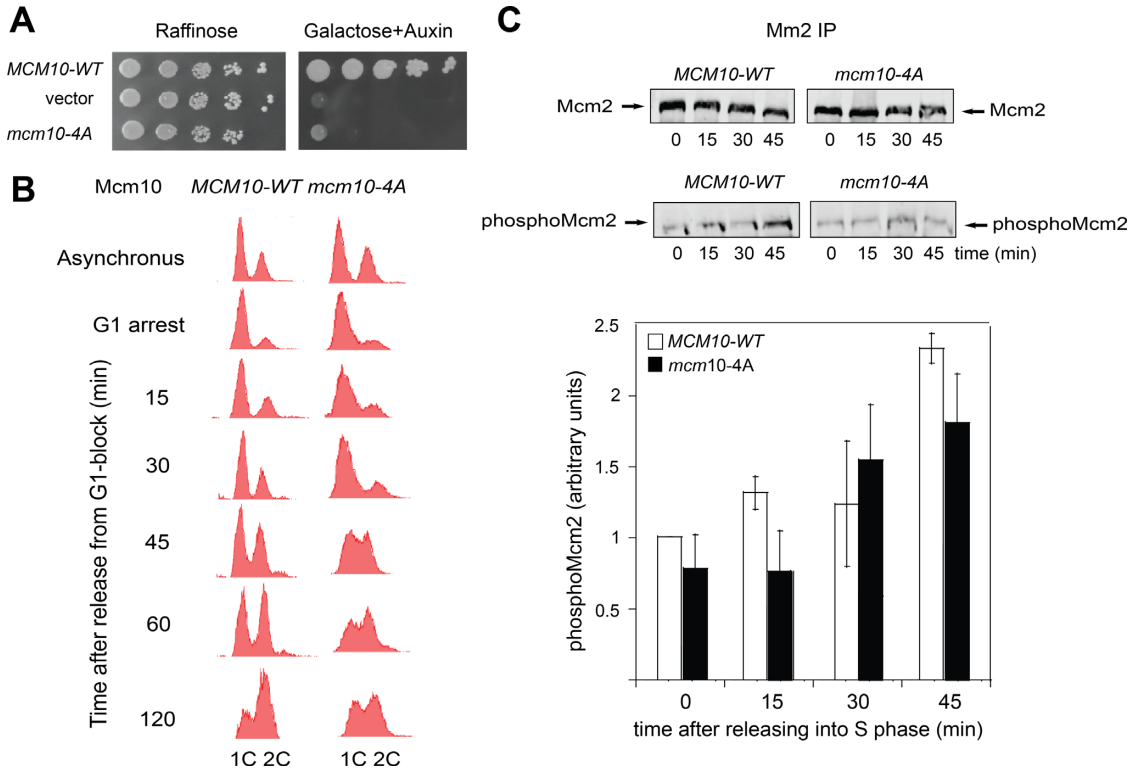

Figure 6. Expression of *mcm10-4A* in budding yeast results in a growth defect and reduced DDK phosphorylation of Mcm2. (**A**) 10-fold serial dilution analysis of budding yeast *mcm10-1*-aid cells expressing MCM10-WT, vector and *mcm10-4A* from the GAL-S plasmid inducible promoter system (pRS415). Plates were incubated for 3 days at 25°C. (**B**) *mcm10-1*-aid cells expressing *MCM10-WT* and *mcm10-4A* were grown as described in Materials and Methods. Cells were analyzed by FACS with propidium iodide staining for DNA content. (**C**) *mcm10-1*-aid cells expressing *MCM10-WT* and *mcm10-4A* were grown as described in Material and Methods. C, upper panel. Mcm2 IP samples were analyzed by western blot for expression of Mcm2. C, bottom panel. Mcm2 IP samples were analyzed by western blot for expression of phospho-Mcm2. Results from similar experiments were quantified, averaged and plotted. Graph from (C) represents mean values from two independent experiments and error bars indicate the standard deviation of the mean.

crease in RPA-ChIP signal, indicating that cells are entering G_2. In contrast, no increase was observed for the non-origin sequence (Figure 7C, right panel). There is a substantial reduction in PCR signal in the case of cells expressing *mcm10-4A* (Figure 7C, left panel). The decrease in RPA-ChIP signal at origins of replication may reflect the importance of the Mcm10 NTD for origin unwinding/melting.

Next, we determined the assembly of CMG in cells expressing *mcm10-4A* in the *mcm5-bob1* background. Cells were synchronized in G_1 with α–factor and then released into medium lacking α–factor for 0, 15, 30 and 45 minutes. We made whole cell extracts and probed them with antibodies against Mcm10, Cdc45, GINS, RPA, Mcm2 and Pol12, using the relevant epitope tags for antigens, and found similar levels of these proteins in cells expressing mutant compared to *wild-type* Mcm10 (Figure 7D, left panel). Then, we immunoprecipitated cells with an antibody against Mcm2 in order to isolate DNA-loaded Mcm2–7 complexes. Levels of Mcm2 were equivalent for cells expressing *mcm10-WT* and *mcm10-4A* (Figure 7D, right panel). We first investigated the interaction between Mcm2–7 and Mcm10 *in vivo* by probing cells with an antibody against Mcm10. We found similar levels of Mcm10 during G_1 and S phase in cells expressing *mcm10-WT* and *mcm10-4A*. This result indicates that the Mcm10-Mcm2–7 interaction is normal in cells expressing *mcm10-4A*. This is consistent with our *in vitro* data in which we showed that Mcm10-4A is able to interact with Mcm2–7 *in vitro* (Figure 3A).

In cells expressing *mcm10-4A,* the level of Cdc45 bound to Mcm2 is similar compared to *wild-type* Mcm10 during S phase (Figure 7D, right panel), indicating that the recruitment of Cdc45 during S phase is normal in cells expressing *mcm10-4A*. In contrast, when we studied the interaction between Mcm2–7 and GINS, we found that there is a reduced signal for GINS-Mcm2–7 interaction in cells expressing *mcm10-4A* (Figure 7D, right panel). This result suggests that GINS assembly with Mcm2–7 is modestly defective during S phase in our Mcm10 NTD mutant.

The role of Mcm10 in CMG assembly is currently a topic of debate. Deleting *MCM10* in previous studies results in either no defect in CMG assembly (26,27,60), or a slight-to-modest defect in CMG assembly, depending upon the study (28,59). Furthermore, CMG can be assembled *in vitro* without any added Mcm10 (9,33,59). The results in the present manuscript show that expression of the *mcm10-4A* mutant results in a modest defect in GINS assembly with Mcm2–7, and this defect is more severe than that observed in our previous study of an *MCM10* deletion (28). Thus, expression of *mcm10-4A* may result in a more severe defect in CMG assembly compared to an *MCM10* deletion. It will be interesting to observe the effect of adding Mcm10-4A to a fully reconstituted *in vitro* DNA replica-

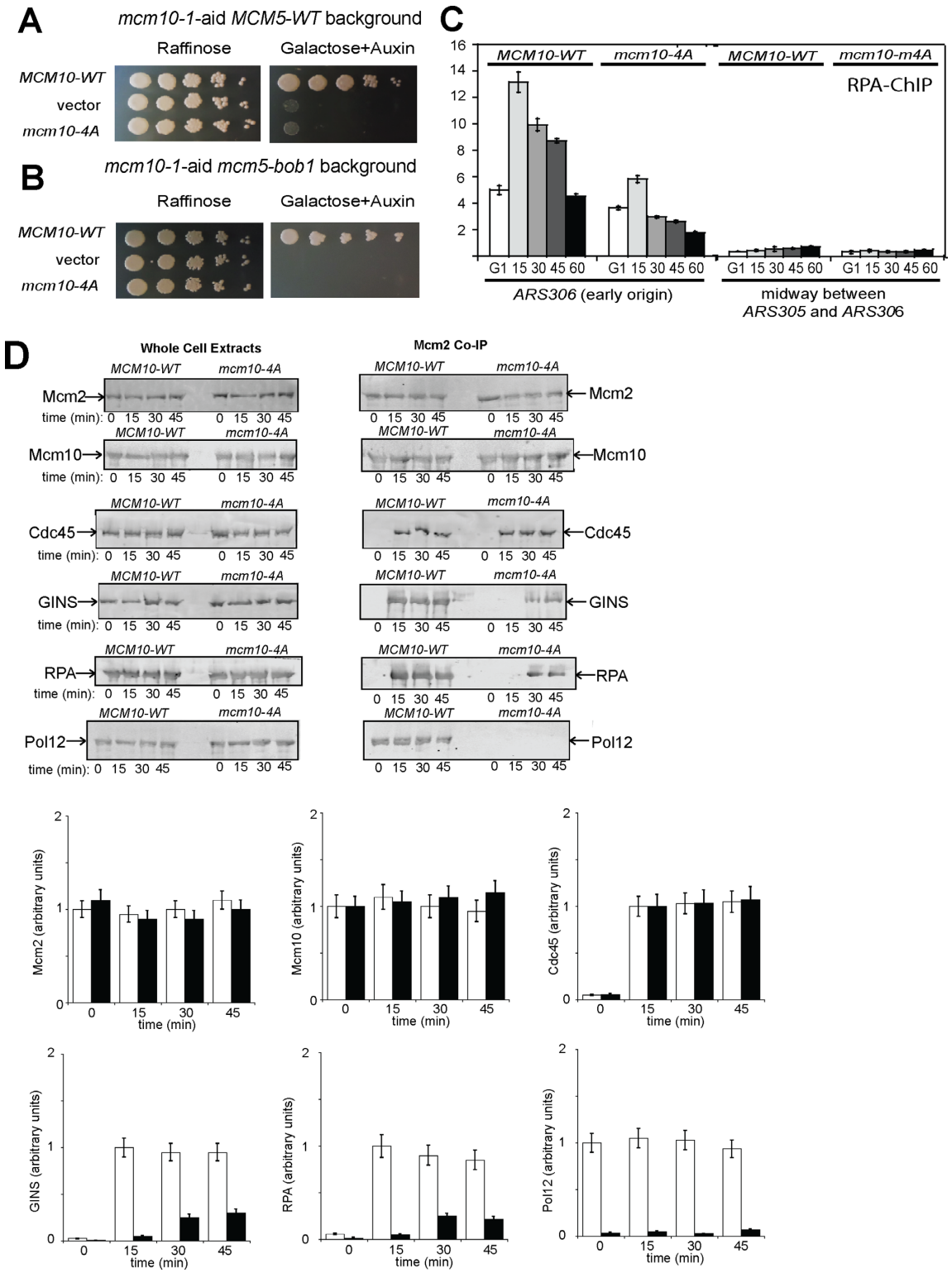

Figure 7. The growth defect observed in cells expressing *mcm10-4A* is not suppressed by the presence of *mcm5-bob1* mutation. (**A**) 10-fold serial dilution analysis of budding yeast *mcm10-1*-aid cells expressing MCM10-WT and *mcm10-4A* from the GAL-S plasmid inducible promoter system (pRS415). Plates were incubated for 3 days at 25°C. (**B**) similar to A, except the cells harbored the *mcm5-bob1* mutation. (**C**) *mcm10-1*-aid *mcm5-bob1* cells expressing *MCM10-WT* and *mcm10-4A* were grown and chromatin immunoprecipitation was performed as described in Materials and Methods. Radioactive PCR bands were quantified, averaged and plotted. (**D**) *mcm10-1*-aid *mcm5-bob1*cells expressing *MCM10-WT* and *mcm10-4A* were grown as described in Materials and Methods. D, left panel. Whole cell extracts were analyzed by Western blot for the expression of the indicated proteins. D, right panel. Cells were immunoprecipitated with antibodies directed against Mcm2 as described in Materials and Methods, followed by western analysis with antibodies directed against Mcm2, Mcm10, Cdc45, GINS, RPA, and Pol12. Results from different experiments were quantified, averaged and plotted. Graphs from (C) and (D) represent mean values from two independent experiments and error bars indicate the standard deviation of the mean.

tion system in the future. We next analyzed the levels of RPA (the *Saccharomyces cerevisiae* ssDNA binding protein) in cells expressing either *MCM10-WT* or *mcm10-4A* by co-immunoprecipitation. We observed that the interaction between RPA and Mcm2 is substantially reduced in cells expressing *mcm10-4A* compared to *MCM10-WT* (Figure 7D, right panel), suggesting that origin unwinding/melting is defective.

A previous study suggested a model in which oligomerization of Mcm10 might be involved in the coordination of both ssDNA and Pol-α interaction at origins of replication (38). We wanted to study the presence of Pol12, a subunit of the Polα primase complex, at origins of replication in cells expressing *mcm10-4A*. We found a substantially reduced Pol12 signal at origins of replication in cells expressing *mcm10-4A* compared to *MCM10-WT*. The presence of two bands for Pol12 is observed because Pol12 is phosphorylated in a cell cycle-specific manner in eukaryotes (61,62).

In summary, the expression of *mcm10-4A* results in the following defects: reduced phosphorylation of Mcm2 by DDK, diminished RPA signal at origins of replication, delayed GINS-Mcm2–7 interaction and defective Polα recruitment to origins of replication.

DISCUSSION

Summary of new results reported in this manuscript

We characterized an Mcm10 mutant that is defective for oligomerization (Mcm10-4A). Using purified proteins, we found that Mcm10-4A is defective in stimulating DDK phosphorylation of Mcm2, binding to 80-nucleotide ssDNA, and recruitment of p180 to Mcm2–7. *In vivo*, we found that expression of *mcm10-4A* resulted in a growth defect as a result of a defective DNA replication and decreased phosphorylation of Mcm2. We also expressed *mcm10-4A* in *mcm5-bob1* cells to suppress the defect resulting from decreased DDK phosphorylation of Mcm2. In the *mcm5-bob1* genetic background, cells expressing *mcm10-4A* exhibited defective growth, decreased association of RPA with origins of replication and decreased recruitment of GINS and pol α to Mcm2–7. We also observed a severe growth defect for cells expressing *mcm10-Δ1-100* that was nearly identical to the growth defect observed for cells expressing *mcm10-4A*. This result differs with reports from other groups using different background strains and methods for depleting endogenous *MCM10*, suggesting that the relative importance of the N-terminus of Mcm10 on cell growth depend upon the background strain and experimental conditions.

In summary, we report the following discoveries in this manuscript that have not been reported elsewhere: (1) An intact Mcm10 coiled-coil interaction surface is important for cell growth. (2) An intact Mcm10 coiled-coil interaction surface is important for Pol12 interaction with Mcm2–7 *in vitro* and *in vivo*. (3) An intact Mcm10 coiled-coil interaction surface is important for RPA recruitment to replication origins *in vivo*, and this defect is correlated to the loss of Mcm10 interaction with single-stranded DNA.

Role of Mcm10 multimerization in origin unwinding

It was previously shown that Mcm10 multimerization is correlated with Mcm10 interaction with long ssDNA (51). Furthermore, it was recently observed that expression of a mutant of Mcm10 defective for ssDNA binding,*mcm10-2,3,4*, results in a substantially diminished RPA-ChIP signal at an origin of replication (29). These previous data suggest that Mcm10 interaction with ssDNA is important for origin melting, perhaps by stabilizing the ssDNA as the melted strand is extruded from the central channel of Mcm2–7 during S phase (29). The DNA binding region of Mcm10 is in the Internal Domain (ID) for budding yeast, while the multimerization domain is in the N-terminal domain (NTD) (36,37). Thus, the mutation reported here, Mcm10-4A, results in decreased interaction with ssDNA because of inhibited Mcm10 multimerization and not because of a direct loss of contact of Mcm10 with ssDNA. Since expression of this Mcm10-multimerization mutation results in decreased RPA-ChIP signal *in vivo*, an intact Mcm10 coiled-coil interaction surface may be important for high affinity of Mcm10 for the melted strand during origin melting in budding yeast (Figure 8A).

Role of Mcm10 multimerization in helicase assembly

We found that expression of *mcm10-4A* results in diminished recruitment of GINS to Mcm2–7 *in vivo*. We previously observed no direct interaction between Mcm10 and GINS (29), suggesting that the diminished helicase assembly reported here is indirect. We have observed similar instances of defective GINS-Mcm2–7 interaction *in vivo* when origin melting is absent (29,50,63,64). The reason for this defect may be that origin melting is important for the efficient interaction between GINS and Mcm2–7 *in vivo*. We previously observed that Sld2 blocks the association of GINS with Mcm2–7, but origin melting sequesters Sld2 form Mcm2–7, allowing GINS to bind Mcm2–7 by a sequestration mechanism (44,49,50). Thus, it is possible that this mechanism is operative when *mcm10-4A* is expressed in budding yeast cells. Thus, according to this model, Mcm10 multimerization is important for binding and stabilization of the melted strand. Then, the melted strand recruits Sld2 away from Mcm2–7, allowing GINS to bind to Mcm2–7 by a passive mechanism (Figure 8B).

Role of Mcm10 multimerization in pol α recruitment to Mcm2–7

Mcm10 is imoportant for the recruitment of pol α to Mcm2–7 during replication initiation (21,31,32). We show here using purified proteins that Mcm10-4A is substantially defective for the recruitment of p180 to Mcm2–7 compared to Mcm10-WT. However, the interaction between Mcm10-4A and both p180 and Mcm2–7 is similar compared to the interaction between Mcm10-WT and p180 and Mcm2–7. Furthermore, expression of *mcm10-4A* in budding yeast cells results in diminished pol α interaction with Mcm2–7 *in vivo*. These data suggest that the multimerization of Mcm10 is important for the recruitment of p180 to Mcm2–7 in budding yeast. We also examined which subunit of Mcm2–7 is important for Mcm10-dependent recruitment of p180 to

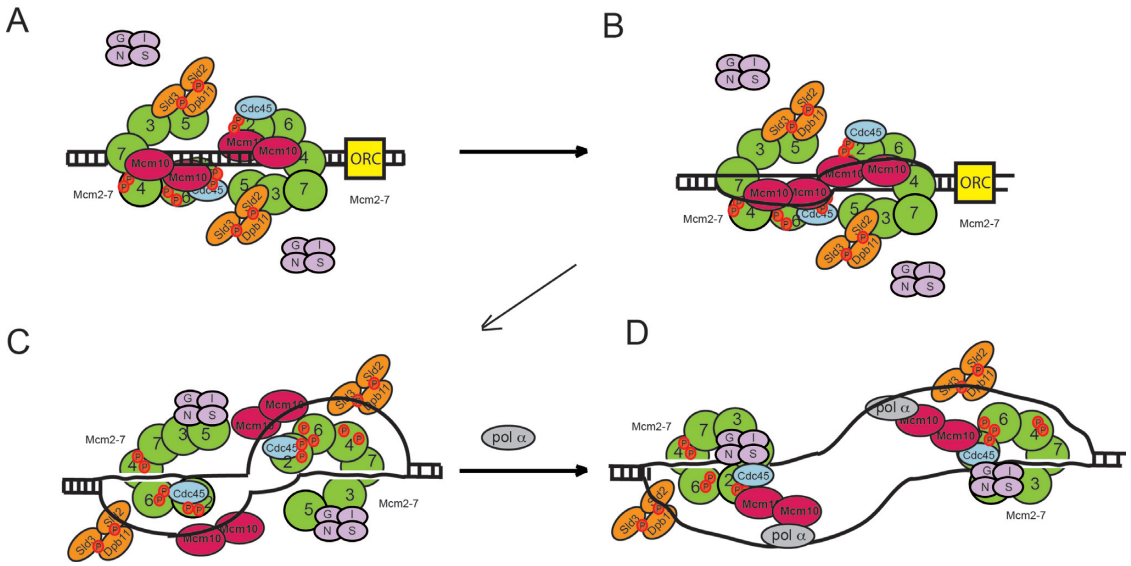

Figure 8. An intact Mcm10 coiled-coil interaction surface is important for origin melting, helicase assembly and the recruitment of Pol-α to Mcm2–7. (**A**) Mcm2–7 complex is loaded as a double hexamer to encircle dsDNA during late M and G_1 phase. In early S phase, Mcm10 stimulates DDK phosphorylation of Mcm2. S-phase cyclin dependent kinase (CDK) phosphorylates Sld2 and Sld3 and these phosphorylated proteins bind to Dpb11 to form the ternary complex Sld3-Sld2-Dpb11 that binds to the Mcm2–7 complex. The Sld3-Sld2-Dpb11 ternary complex blocks the interaction between GINS and Mcm2–7. Lagging stand ssDNA is extruded from the central ring of Mcm2–7 complex. (**B**) Mcm10 oligomerization promotes Mcm10-binding to the extruded lagging ssDNA strand. (**C**) Sld3-Sld2-Dpb11 bind to the melted, lagging ssDNA strand, allowing GINS to bind Mcm2–7 by a passive, sequestration mechanism. (**D**) Mcm10 oligomerization promotes the recruitment of pol α to Mcm2–7.

Mcm2–7 and found that Mcm2 interaction with p180 is substantially dependent on Mcm10 multimerization, while Mcm4 and Mcm7 are modestly dependent. These data suggest that Mcm10 may recruit p180 to Mcm2–7 by directly interaction with Mcm2 and p180. We propose that one subunit of Mcm10 binds to Mcm2, a second Mcm10 subunit binds to p180 and the formation of a dimer between these two Mcm10 subunits confers the efficient recruitment of pol α to Mcm2–7 during DNA replication initiation (Figure 8C).

SUPPLEMENTARY DATA

Supplementary Data are available at NAR Online.

ACKNOWLEDGEMENTS

We thank Cheryl Pye and Brian Washburn from FSU Molecular Cloning Facility for helping with cloning and mutant constructs. We thank Ryan Higgins and Dr Yanchang Wang for their help in the construction of *mcm10-1*-aid *mcm5-bob1* strain. We thank Yeast Genetic Resource Center for providing *mcm10-1*-aid reagents, Robert A. Sclafani for *mcm5-bob1* strain and Susan Taylor for supplying purified PKA. We also thank Ruth Didier for help with FACS analysis and Dr Yoichi Kato for the use of his sonicator.

FUNDING

National Institute of General Medical Sciences of the National Institutes of Health [R15GM113167 to D.L.K.]. Funding for open access charge: National Institute of General Medical Sciences of the National Institutes of Health [R15GM113167 to D.L.K.].

Conflict of interest statement. None declared.

REFERENCES

1. Remus,D., Beuron,F., Tolun,G., Griffith,J., Morris,E. and Diffley,J. (2009) Concerted loading of Mcm2–7 double hexamers around DNA during DNA replication origin licensing. *Cell*, **139**, 719–730.
2. Evrin,C., Clarke,P., Zech,J., Lurz,R., Sun,J., Uhle,S., Li,H., Stillman,B. and Speck,C. (2009) A double-hexameric MCM2-7 complex is loaded onto origin DNA during licensing of eukaryotic DNA replication. *Proc. Natl. Acad. Sci. U.S.A.*, **106**, 20240–20245.
3. Gambus,A., Khoudoli,G., Jones,R. and Blow,J. (2011) MCM2-7 form double hexamers at licensed origins in Xenopus egg extract. *J. Biol. Chem.*, **286**, 11855–11864.
4. Labib,K. (2010) How do Cdc7 and cyclin-dependent kinases trigger the initiation of chromosome replication in eukaryotic cells? *Genes Dev.*, **24**, 1208–1219.
5. Costa,A., llves,I., Tamberg,N., Petojevic,T., Nogales,E., Botchan,M. and Berger,J. (2011) The structural basis for MCM2-7 helicase activation by GINS and Cdc45. *Nat. Struct. Mol. Biol.*, **18**, 471–477.
6. Moyer,S., Lewis,P. and Botchan,M. (2006) Isolation of the Cdc45/Mcm2–7/GINS (CMG) complex, a candidate for the eukaryotic DNA replication fork helicase. *Proc. Natl. Acad. Sci. U.S.A.*, **103**, 10236–10241.
7. Ilves,I., Petojevic,T., Pesavento,J. and Botchan,M. (2010) Activation of the MCM2-7 helicase by association with Cdc45 and GINS proteins. *Mol. Cell*, **37**, 247–258.
8. Gambus,A., Jones,R.C., Sanchez-Diaz,A., Kanemaki,M., Deursen,F.v., Edmondson,R.D. and Labib,K. (2006) GINS maintains association of Cdc45 with MCM in replisome progression complexes at eukaryotic DNA replication forks. *Nat. Cell Biol.*, **8**, 358–366.
9. Yeeles,J., Deegan,T., Janska,A., Early,A. and Diffley,J. (2015) Regulated eukaryotic DNA replication origin firing with purified proteins. *Nature*, **519**, 431–435.
10. Lydeard,J.R., Lipkin-Moore,Z., Sheu,Y.-J., Stillman,B., Burgers,P.M. and Haber,J.E. (2010) Break-induced replication requires all essential DNA replication factors except those specific for pre-RC assembly. *Genes Dev.*, **24**, 1133–1144.

11. Masai,H., Taniyama,C., Ogino,K., Matsui,E., Kakusho,N., Matsumoto,S., Kim,J., Ishii,A., Tanaka,T., Kobayashi,T. *et al.* (2006) Phosphorylation of MCM4 by Cdc7 kinase facilitates its interaction with Cdc45 on the chromatin. *J. Biol. Chem.*, **281**, 39249–39261.
12. Lei,M., Kawasaki,Y., Young,M., Kihara,M., Sugino,A. and Tye,B. (1997) MCM2 is a target of regulation by Cdc7-Dbf4 during the initiation of DNA synthesis. *Genes Dev.*, **11**, 3365–3374.
13. Bruck,I. and Kaplan,D. (2009) Dbf4-Cdc7 phosphorylation of Mcm2 is required for cell growth. *J. Biol. Chem.*, **284**, 28823–28831.
14. Bruck,I. and Kaplan,D.L. (2015) The Dbf4-Cdc7 kinase promotes Mcm2–7 ring opening to allow for single-stranded DNA extrusion and helicase assembly. *J. Biol. Chem.*, **290**, 1210–1221.
15. Fu,Y., Yardimci,H., Long,D., Ho,T., Guainazzi,A., Bermudez,V., Hurwitz,J., van Oijen,A., Schärer,O. and Walter,J. (2011) Selective bypass of a lagging strand roadblock by the eukaryotic replicative DNA helicase. *Cell* **146**, 931–941.
16. Kaplan,D.L., Davey,M.J. and O'Donnell,M. (2003) Mcm4,6,7 uses a 'pump in ring' mechanism to unwind DNA by steric exclusion and actively translocate along a duplex. *J. Biol. Chem.*, **278**, 49171–49182.
17. Solomon,N., Wright,M., Chang,S., Buckley,A., Dumas,L. and Gaber,R. (1992) Genetic and molecular analysis of DNA43 and DNA52: two new cell-cycle genes in Saccharomyces cerevisiae. *Yeast*, **8**, 273–289.
18. Merchant,A., Kawasaki,Y., Chen,Y., Lei,M. and Tye,B.K. (1997) A lesion in the DNA replication initiation factor Mcm10 induces pausing of elongation forks through chromosomal replication origins in S. cerevisiae. *Mol. Cell. Biol.*, **17**, 3261–3271.
19. Thu,Y. and Bielinsky,A. (2013) Enigmatic rles of Mcm10 in DNA replication. *Trends Biochem. Sci.*, **38**, 184–194.
20. Thu,Y. and Bielinsky,A. (2014) MCM10: one tool for all-Integrity, maintenance and damage control. *Semin. Cell Dev. Biol.*, **30**, 121–130.
21. Ricke,R.M. and Bielinsky,A.K. (2004) Mcm10 regulates the stability and chromatin association of DNA polymerase-alpha. *Mol. Cell*, **16**, 173–185. .
22. Douglas,M. and Diffley,J. (2016) Recruitment of Mcm10 to sites of replication initiation requires direct binding to the MCM complex. *J. Biol. Chem*, **291**, 5879–5888.
23. Aparicio,O.M., Weinstein,D.M. and Bell,S.P. (1997) Components and dynamics of DNA replication complexes in S. cerevisiae: redistribution of MCM proteins and Cdc45p during S phase. *Cell*, **91**, 59–69.
24. Zou,L. and Stillman,B. (2000) Assembly of a complex containing Cdc45p, replication protein A, and Mcm2p at replication origins controlled by S-phase cyclin-dependent kinases and Cdc7p-Dbf4p kinase. *Mol. Cell. Biol.*, **20**, 3086–3096.
25. Handa,T., Kanke,M., Takahashi,T., Nakagawa,T. and Masukata,H. (2012) DNA polymerization-independent functions of DNA polymerase epsilon in assembly and progression of the replisome in fission yeast. *Mol. Biol. Cell.* , **23**, 3240–3253.
26. van Deursen,F., Sengupta,S., De Piccoli,G., Sanchez-Diaz,A. and Labib,K. (2012) Mcm10 associates with the loaded DNA helicase at replication origins and defines a novel step in its activation. *EMBO J.*, **31**, 2195–2206.
27. Watase,G., Takisawa,H. and Kanemaki,M. (2012) Mcm10 plays a role in functioning of the eukaryotic replicative DNA helicase, Cdc45-Mcm-GINS. *Curr. Biol.*, **22**, 343–349.
28. Perez-Arnaiz,P., Bruck,I. and Kaplan,D. (2016) Mcm10 coordinates the timely assembly and activation of the replication fork helicase. *Nucleic Acids Res.* , **44**, 315–329.
29. Perez-Arnaiz,P. and Kaplan,D. (2016) An Mcm10 mutant defective in ssDNA binding shows defects in DNA replication initiation. *J. Mol. Biol.*, **428**, 4608–4625.
30. Wohlschlegel,J., Dhar,S., Prokhorova,T., Dutta,A. and Walter,J. (2002) Xenopus Mcm10 binds to origins of DNA replication after Mcm2–7 and stimulates origin binding of Cdc45. *Mol. Cell*, **9**, 233–240.
31. Ricke,R. and Bielinsky,A. (2006) A conserved Hsp10-like domain in Mcm10 is required to stabilize the catalytic subunit of DNA polymerase-alpha in budding yeast. *J. Biol. Chem.*, **281**, 18414–18425.
32. Zhu,W., Ukomadu,C., Jha,S., Senga,T., Dhar,S., Wohlschlegel,J., Nutt,L., Kornbluth,S. and Dutta,A. (2007) Mcm10 and And-1/CTF4 recruit DNA polymerase alpha to chromatin for initiation of DNA replication. *Genes Dev.*, **21**, 2288–2299.
33. Heller,R., Kang,S., Lam,W., Chen,S., Chan,C. and Bell,S. (2011) Eukaryotic origin-dependent DNA replication in vitro reveals sequential action of DDK and S-CDK kinases. *Cell*, **146**, 80–91.
34. Robertson,P., Warren,E., Zhang,H., Friedman,D., Lary,J., Cole,J., Tutter,A., Walter,J., Fanning,E. and Eichman,B. (2008) Domain architecture and biochemical characterization of vertebrate Mcm10. *J. Biol. Chem.* , **283**, 3338–3348.
35. Du,W., Stauffer,M. and Eichman,B. (2012) Structural biology of replication initiation factor Mcm10. *Subcell Biochem.*, **62**, 197–216.
36. Du,W., Josephrajan,A., Adhikary,S., Bowles,T., Bielinsky,A. and Eichman,B. (2013) Mcm10 self-association is mediated by an N-terminal coiled-coil domain. *PLoS One*, **8**, e70518.
37. Warren,E., Vaithiyalingam,S., Haworth,J., Greer,B., Bielinsky,A., Chazin,W. and Eichman,B. (2008) Structural basis for DNA binding by replication initiator Mcm10. *Structure*, **16**, 1892–1901.
38. Warren,E., Huang,H., Fanning,E., Chazin,W. and Eichman,B. (2009) Physical interactions between Mcm10, DNA, and DNA polymerase alpha. *J. Biol. Chem.*, **284**, 24662–24672.
39. Das-Bradoo,S., Ricke,R.M. and Bielinsky,A.K. (2006) Interaction between PCNA and diubiquitinated Mcm10 is essential for cell growth in budding yeast. *Mol. Cell. Biol.*, **26**, 4806–4817.
40. Lee,J., Seo,Y. and Hurwitz,J. (2003) The Cdc23 (Mcm10) protein is required for the phosphorylation of minichromosome maintenance complex by the Dfp1-Hsk1 kinase. *Proc. Natl. Acad. Sci. U.S.A.*, **100**, 2334–2339.
41. Di Perna,R., Aria,V., De Falco,M., Sannino,V., Okorokov,A., Pisani,F. and De Felice,M. (2013) The physical interaction of Mcm10 with Cdc45 modulates their DNA-binding properties. *Biochem. J.* , **454**, 333–343.
42. Okorokov,A.L., Waugh,A., Hodgkinson,J., Murthy,A., Hong,H.K., Leo,E., Sherman,M.B., Stoeber,K., Orlova,E.V. and Williams,G.H. (2007) Hexameric ring structure of human MCM10 DNA replication factor. *EMBO Rep.*, **8**, 925–930.
43. Alver,R., Zhang,T., Josephrajan,A., Fultz,B., Hendrix,C., Das-Bradoo,S. and Bielinsky,A. (2014) The N-terminus of Mcm10 is important for interaction with the 9-1-1 clamp and in resistance to DNA damage. *Nucleic Acids Res.*, **42**, 8389–8404.
44. Kanter,D. and Kaplan,D. (2011) Sld2 binds to origin single-stranded DNA and stimulates DNA annealing. *Nucleic Acids Res.*, **39**, 2580–2592.
45. Bruck,I. and Kaplan,D. (2013) Cdc45 protein-single-stranded DNA interaction is important for stalling the helicase during replication stress. *J. Biol. Chem.*, **288**, 7550–7563.
46. Davey,M.J., Indiani,C. and O'Donnell,M. (2003) Reconstitution of the Mcm2–7p heterohexamer, subunit arrangement, and ATP site architecture. *J. Biol. Chem.*, **278**, 4491–4499.
47. Sclafani,R., Tecklenburg,M. and Pierce,A. (2002) The mcm5-bob1 bypass of Cdc7p/Dbf4p in DNA replication depends on both Cdk-1 independent and Cdk-1-dependent steps in Saccharomyces cerevisiae. *Genetics*, **161**, 47–57.
48. Gietz,R. and Woods,R. (2002) Transformation of yeast by lithium acetate/single-stranded carrier DNA/polyethylene glycol method. *Methods Enzymol.*, **350**, 87–96.
49. Bruck,I., Kanter,D.M. and Kaplan,D.L. (2011) Enabling association of the GINS tetramer with the Mcm2–7 complex by phosphorylated Sld2 protein and single-stranded origin DNA. *J. Biol. Chem.*, **286**, 36414–36426.
50. Bruck,I. and Kaplan,D. (2014) The replication initiation protein sld2 regulates helicase assembly. *J. Biol. Chem.*, **289**, 1948–1959.
51. Eisenberg,S., Korza,G., Carson,J., Liachko,I. and Tye,B. (2009) Novel DNA binding properties of the Mcm10 protein from Saccharomyces cerevisiae. *J. Biol. Chem.*, **284**, 25412–25420.
52. Quan,Y., Xia,Y., Liu,L., Cui,J., Li,Z., Cao,Q., Chen,X., Campbell,J. and Lou,H. (2015) Cell-cycle-regulated interaction between Mcm10 and double hexameric Mcm2–7 is required for helicase splitting and activation during S phase. *Cell Rep.*, **13**, 2576–2586.
53. Gregan,J., Lindner,K., Brimage,L., Franklin,R., Namdar,M., Hart,E., Aves,S. and Kearsey,S. (2003) Fission yeast Cdc23/Mcm10 functions after pre-replicative complex formation to promote Cdc45 chromatin binding. *Mol. Biol. Cell*, **14**, 3876–3887.

54. Sawyer,S., Cheng,I., Chai,W. and Tye,B. (2004) Mcm10 and Cdc45 cooperate in origin activation in Saccharomyces cerevisiae. *J. Mol. Biol.*, **340**, 195–202.
55. Biswas,S., Khopde,S., Zhu,F.F. and Biswas,E. (2003) Subunit interactions in the assembly of Saccharomyces cerevisiae DNA polymerase alpha. *Nucleic Acids Res.*, **31**, 2056–2065.
56. Nishimura,K., Fukagawa,T., Takisawa,H., Kakimoto,T. and Kanemaki,M. (2009) An auxin-based degron system for the rapid depletion of proteins in nonplant cells. *Nat. Methods.*, **6**, 917–922.
57. Mumberg,D., Müller,R. and Funk,M. (1994) Regulatable promoters of Saccharomyces cerevisiae: comparison of transcriptional activity and their use for heterologous expression. *Nucleic Acids Res.*, **22**, 5767–5768.
58. Hardy,C.F.J., Dryga,O., Seematter,S., Pahl,P.M.B. and Sclafani,R.A. (1997) *mcm5/cdc46-bob1* bypasses the requirement for the S phase activatorCdc7p. *Proc. Natl. Acad. Sci. U.S.A.*, **94**, 3151–3155.
59. Lõoke,M., Maloney,M.F. and Bell,S.P. (2017) Mcm10 regulates DNA replication elongation by stimulating the CMG replicative helicase. *Genes Dev.*, **31**, 291–305.
60. Kanke,M., Kodama,Y., Takahashi,T., Nakagawa,T. and Masukata,H. (2012) Mcm10 plays an essential role in origin DNA unwinding after loading of the CMG components. *EMBO J.*, **31**, 2182–2194.
61. Ferrari,M., Lucchini,G., Plevani,P. and Foiani,M. (1996) Phosphorylation of the DNA polymerase alpha-primase B subunit is dependent on its association with the p180 polypeptide. *J. Biol. Chem.*, **70**, 8661–8666.
62. Voitenleitner,C., Rehfuess,C., Hilmes,M., O'Rear,L., Liao,P., Gage,D., Ott,R., Nasheuer,H. and Fanning,E. (1999) Cell cycle-dependent regulation of human DNA polymerase alpha-primase activity by phosphorylation. *Mol. Cell. Biol.*, **19**, 646–656.
63. Bruck,I. and Kaplan,D. (2015) The replication initiation protein Sld3/Treslin orchestrates the assembly of the replication fork helicase during S phase. *J. Biol. Chem.*, **290**, 27414–27424.
64. Dhingra,N., Bruck,I., Smith,S., Ning,B. and Kaplan,D. (2015) Dpb11 helps control assembly of the Cdc45-Mcm2–7-GINS replication fork helicase. *J. Biol. Chem.*, **290**, 7586–7601.